PHYSICAL REVIEW D VOLUME 46, NUMBER 9 1 NOVEMBER 1992

Fermion masses in SO(10)

Gerard Jungman*
Enrico Fermi Institute and Department of Physics, University of Chicago, 5640 S. Ellis Avenue, Chicago, Illinois 60637
(Received 18 February 1992)

Yukawa-coupling-constant unification together with the known fermion masses is used to constrain SO(10) models. We consider the case of one (heavy) generation, with the tree-level relation $m_b = m_\tau$, calculating the limits on the intermediate scales due to the known limits on fermion masses. This analysis extends previous analyses which addressed only the simplest symmetry-breaking schemes. In the case where the low-energy model is the standard model with one Higgs doublet, there are very strong constraints due to the known limits on the top-quark mass and the τ-neutrino mass. The two-Higgs-doublet case is less constrained, though we can make progress in constraining this model also. We identify those parameters to which the viability of the model is most sensitive. We also discuss the "triviality" bounds on m_t obtained from the analysis of the Yukawa renormalization-group equations. Finally we address the role of a speculative constraint on the τ-neutrino mass, arising from the cosmological implications of anomalous $B+L$ violation in the early Universe.

PACS number(s): 12.10.Dm, 12.15.Ff

I. INTRODUCTION

Two major factors have led to a recent revival of interest in the renormalization-group calculations associated with grand-unified gauge theories. The first factor is the increasing precision of coupling-constant measurements at the Z resonance [1]. New calculations of gauge coupling unification have reduced the viability of some unification schemes and perhaps enhanced the attractiveness of others [2,3]. The second factor is the increasing lower bound on the top-quark mass from direct searches [4]. Yukawa-coupling-constant unification makes a heavy top quark difficult to accept in some models, and calculations have shown how an upper bound on m_t lower than those from the so-called "triviality bound" or from the ρ-parameter constraint can arise in SO(10) models with the simplest viable symmetry-breaking scheme [5,6].

The purpose of this paper is to analyze the unification of Yukawa couplings in the SO(10) theory for symmetry-breaking schemes more general than those previously considered. In particular, we separate the scales of $SU(2)_R$ breaking and $U(1)_{I_{3R}}$ breaking. Using the known bounds on the mass of the top quark and the mass of the τ neutrino, we are able to eliminate large regions of parameter space for the model. The original motivation for this work was to understand in detail the consequences of a certain speculative neutrino mass bound discussed previously [7,8]. Thus, we devote a section to a discussion of this bound and its manifestation in SO(10). We assume the tree-level relation $m_b = m_\tau$, corresponding to a Yukawa coupling of the fermion multiplet to the scalar **10** of SO(10). This is not the most general relation, but the complications are great enough that we leave the general case for later work. In particular, the analysis of the scalar-**126** Yukawa case, with the general tree-level relation, is in progress [9]. Once we have a quantitative understanding of these cases we hope to perform a similar analysis for the generic mixed case, with the machinery described herein.

For definiteness we have settled on a particular set of Higgs representations. The analysis here is easily extended to others, but we have chosen to consider only those representations introduced below. However, the set of "small" useful representations is not that large, and future work can reproduce our renormalization-group calculations for this handful of interesting cases if it becomes crucial to the analysis of SO(10).

II. SYMMETRY-BREAKING SCHEMES

In this section we review the Higgs representations that we will consider, the symmetry-breaking schemes which they will allow, the branching rules for these representations with respect to the various chains of unbroken subgroups, which give the content of the Higgs representations in the intermediate theories, and the Yukawa couplings of these Higgs representations. None of this material is new [10].

Recall that each generation of fermions in the SO(10) theory resides in a spinorial **16** of SO(10), with the requisite addition of a right-handed neutrino. Therefore, possible Yukawa-coupled Higgs representations must lie in $\mathbf{16}\otimes\mathbf{16}=\mathbf{10}_{\rm sym}\oplus\mathbf{120}_{\rm asym}\oplus\mathbf{126}$. The **120** is antisymmetric and thus contributes only to intergenerational mixing. Since we will be concerned here only with the one-generation model (the top generation), we will ignore the Yukawa couplings of the **120**. Thus there are two independent Yukawa couplings at the SO(10) unification scale.

The phenomenologically viable breaking of SO(10) is to

*Electronic address: jungman@yukawa.uchicago.edu

the maximal subalgebra SU(2)×SU(2)×SU(4), one SU(2) factor being identified as the weak isospin group, the other being right isospin, breaking to a U(1) of I_{3R}; the SU(4) breaks to $SU(3)_{color}\times U(1)_{B-L}$ [11]. The case of intermediate SU(5) symmetry is ruled out by the nonobservation of proton decay combined with current measurements of $\sin^2\theta_W$. We use the notation

$$\begin{aligned}
G_{224}&=SU(2)_L\times SU(2)_R\times SU(4)_c\ ,\\
G_{2213}&=SU(2)_L\times SU(2)_R\times U(1)_{B-L}\times SU(3)_c\ ,\\
G_{214}&=SU(2)_L\times U(1)_{I_{3R}}\times SU(4)_c\ ,\\
G_{2113}&=SU(2)_L\times U(1)_{I_{3R}}\times U(1)_{B-L}\times SU(3)_c\ ,\\
G_{213}&=SU(2)_L\times U(1)_Y\times SU(3)_c\ .
\end{aligned} \tag{2.1}$$

There are two symmetry-breaking chains:

$$\begin{aligned}
&G_{224}\xrightarrow{M_{R_+}}G_{214}\xrightarrow{M_c}G_{2113}\xrightarrow{M_{R_0}}G_{213}\ ,\\
&G_{224}\xrightarrow{M_c}G_{2213}\xrightarrow{M_{R_+}}G_{2113}\xrightarrow{M_{R_0}}G_{213}\ .
\end{aligned} \tag{2.2}$$

These chains can be induced by the Higgs representations **10**, **45**, **54**, **126**, and **210**. Listed in Table I are the branchings of these representations with respect to the various subgroups. The minimal fine-tuning and extended survival hypotheses [12] have been invoked in order to eliminate many Higgs representations in the lower-energy effective theories. Simply stated, scalars which do not need to be light are not, and this property is arguably natural since it involves a minimal fine-tuning of the scalar potential [13].

In each of the two symmetry-breaking chains, the **54** breaks SO(10) to G_{224}. In the first chain, the **(1,1,15)** breaks $SU(4)_c$ down to $SU(3)_c\times U(1)_{B-L}$; then the $(\mathbf{1,3,1})_0$ breaks $SU(2)_R$ to $U(1)_{I_{3R}}$. Finally the $(\mathbf{1,1})_{2,\pm1}$ breaks both I_{3R} and $B-L$, leaving unbroken the linear combination which is hypercharge; it is at this point that lepton number is spontaneously broken, and the right-handed neutrino acquires a Majorana mass and is subsequently integrated out. In the second chain, the **(1,3,1)** first breaks $SU(2)_R$; then the **(1,15)** breaks $SU(4)_c$. Again the $(\mathbf{1,1})_{2,\pm1}$ breaks both I_{3R} and $B-L$ to hypercharge.

By choosing a representation other than the **54** to break SO(10), it is possible to also break the *D*-parity symmetry, which forces the $SU(2)_L$ and $SU(2)_R$ coupling constants to be the same down to the $SU(2)_R$-breaking scale [14]. This symmetry breaking manifests itself through unequal scalar contributions to the running of the left-handed and right-handed gauge couplings. We will review the merits of this M_u-scale *D*-parity breaking below.

TABLE I. Higgs representations present at each intermediate stage of symmetry breaking. The top row shows the SO(10) representation from which they descend. For the G_{2113} theory the Abelian quantum numbers are listed $(\cdots)_{B-L,I_{3R}}$. For the theories with $SU(2)_R$ symmetry and with *D* parity broken at the SO(10) scale, the right-handed triplet representations are omitted from the spectrum. Notice that the **54** does not appear in the Table since its function is solely to break SO(10), and after accomplishing this it disappears from the spectrum since, by hypothesis, it has a mass on the order of this breaking scale.

	210	45	126	10
G_{224}	**(1,1,15)**	**(1,3,1)**	**(1,3,10)**	**(2,2,1)**
		(3,1,1)	$(\mathbf{3,1},\overline{\mathbf{10}})$	
G_{214}		$(\mathbf{1,15})_0$	$(\mathbf{1,10})_{\pm1}$	$(\mathbf{2,1})_{\pm1}$
G_{2213}		$(\mathbf{1,3,1})_0$	$(\mathbf{1,3,1})_2$	$(\mathbf{2,1,1})_0$
		$(\mathbf{3,1,1})_0$	$(\mathbf{3,1,1})_2$	
G_{2113}			$(\mathbf{1,1})_{2,\pm1}$	$(\mathbf{2,1})_{0,\pm1}$
G_{213}				$(\mathbf{2,1})_{\pm1}$

III. GAUGE-COUPLING EVOLUTION AND INTERMEDIATE SCALES

The first step is to solve the renormalization-group (RG) equations for the gauge couplings. This analysis has been carried out previously [15,14] at various levels of sophistication since the SO(10) model was introduced. Our procedure in the analysis of the gauge-coupling evolution is to express two of the intermediate scales in terms of the other two scales and the measured values of the gauge couplings at low energies. This information can then be applied directly to the Yukawa-coupling evolution which is our interest here.

We use the one-loop β functions for the gauge couplings, and we include the effects of the scalars in the gauge-coupling β functions. Note that we have specified particular representations, and by invoking the minimal fine-tuning and extended survival hypotheses we remove any ambiguities with regard to the scalar thresholds. However, this is only a prescription, and as has been pointed out previously [16], a two-loop analysis can be a waste of effort without a good reason to believe in the appropriateness of some particular scalar mass values and a particular content of the representations at higher scales. Also, the two-loop effects are generically small unless the $SU(4)_c$ symmetry survives to low scales [14]. This does not occur in our models because we assume that *D*-parity breaking, if it occurs, will occur at the SO(10)-breaking scale, and because the observed value of $\sin^2\theta_W$ does not allow it, as we will see below.

There are several external constraints on the intermediate scales. The first is the constraint that the proton lifetime be greater than the observed bound, $\tau_p>5.5\times10^{32}$ yr [17]. A calculation of the lifetime [18] gives

$$\tau_p=(1-40)\times10^{31}\ \text{yr}\left[\frac{M_u}{10^{15}\ \text{GeV}}\right]^4 , \tag{3.1}$$

so we must require $M_u\gtrsim1.1\times10^{15}$ GeV. Also, the choice of scale for $SU(2)_R$ breaking can have important cosmological consequences. For example, in order to explain the observed baryon asymmetry of the Universe, it has been shown [19], in the case where *D* parity is unbroken above M_{R_+}, that M_{R_+} must be at least as big as 10^{12} GeV. However, when *D* parity breaks well above this scale, this lower bound on M_{R_+} disappears [14]. This is one of the merits of M_u-scale D-parity breaking. Furthermore, without implementation of M_u-scale D-parity breaking, one may be forced to fine-tune the scalar potential in order to avoid upsetting the standard neutrino mass seesaw [20]. As we will see below, the D-parity breaking of the models has little effect on the Yukawa-coupling evolution, and so we relax the above bound on M_{R_+} without introduction of extra complication.

Recall [21] that the running coupling of an SU(N) gauge theory obeys the RG equation

$$2\pi\mu\frac{d}{d\mu}(\alpha^{-1})=\tfrac{11}{3}N-\tfrac{4}{3}n_G-\tfrac{1}{6}S\ , \tag{3.2}$$

where $\alpha=g^2/4\pi, n_G$ is the number of generations of Dirac fermions, and S is the quadratic Casimir constant for the scalar representation, $\mathrm{tr}(\theta^a\theta^b)=S\delta^{ab}$. Solving these with imposition of the unification boundary conditions gives the following relations between the various mass scales and low-energy couplings, analogous to the relations derived in [15]:

$$\alpha(M_Z)^{-1}-\tfrac{8}{3}\alpha_3(M_Z)^{-1}=\frac{11}{3\pi}\ln(x_u^{2+p_u}x_+^{1+p_+}x_0^{p_0}x_c^{p_c})\ , \tag{3.3}$$

$$\alpha(M_Z)^{-1}(3-8\sin^2\theta_W)=\frac{11}{3\pi}\ln(x_u^{-2+q_u}x_+^{3+q_+}x_0^{q_0}x_c^{4+q_c})\ . \tag{3.4}$$

Here, $x_i=M_{R_i}/M_W$. The exponents p_i and q_i are "small" in the sense that they vanish when the scalars are not included in the analysis. The expressions for the exponents as functions of the Higgs-representation quadratic Casimir constants are given in Appendix A, along with some discussion as to their typical values. The dependence on M_{R_0} is slight, so that this scale is essentially free, subject to the obvious constraint $M_{R_0}<M_{R_+}$. The exponents q_c and q_+ are directly relevant to the program of Yukawa-coupling unification since they change the determination of the intermediate scales at which Yukawa couplings unify and these exponents are larger than one might have expected due to the large dimensions of the scalar representations at these higher scales.

As independent parameters to be input, we choose the strong and electromagnetic gauge couplings at the Z pole, $\alpha_3(M_Z),\alpha(M_Z)$, the Weinberg angle $\sin^2\theta_W$, and the intermediate scales M_{R_+} and M_{R_0}. From this information, using (3.3) and (3.4), we can calculate the other intermediate scales M_u and M_c. As an illustration of the effect of the scalars on the calculation, consider Fig. 1, where we plot M_u and M_c as a function of M_{R_+} and M_{R_0} for fixed values of the other parameters. The solid lines show these relations when the scalars are removed from the analysis. The broken lines show the relations when the scalars are included, both with and without D-parity breaking at the SO(10)-breaking scale. By varying M_{R_0}, these broken curves can be shifted very slightly, corresponding to the very slight dependence on M_{R_0} in (3.3) and (3.4). For example, in varying M_{R_0} over the range 10^5 GeV $<M_{R_0}<M_{R_+}$, the predictions for M_c and M_u vary by a factor $\simeq 1.2$. From Fig. 1 we also see that the models imply a lower limit on the right-handed breaking scale, $M_{R_+}\gtrsim 10^9$ GeV, since values less than that would imply $M_c>M_u$.

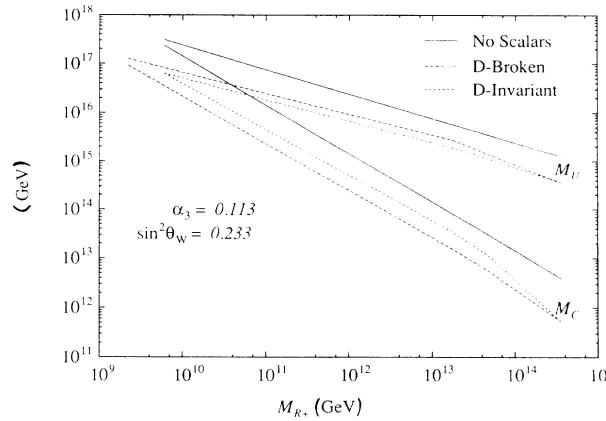

FIG. 1. Intermediate scales M_u and M_c as a function of the scale M_{R_+}; as discussed in the text, the dependence on M_{R_0} is very slight. This illustrates three cases: D parity broken at M_u, no D-parity breaking above M_{R_+}, and no scalar contributions at all.

Notice that the value of M_c can decrease by approximately an order of magnitude when the scalars are included, keeping the other parameters fixed. Since the boundary condition for the Yukawa-coupling evolution is set at M_c, this evolution is sensitive to the presence of the scalars. M_u and M_c decrease when the scalars are introduced because of the effect of the scalars on the running of the Abelian couplings. The effect on the non-Abelian couplings is to slow down their evolution, making them "less" asymptotically free, but the effect on the Abelian couplings is to speed their evolution. It turns out that the effect of the scalar representations on the latter is more important, and thus M_u and M_c are brought downward.

IV. YUKAWA-COUPLING EVOLUTION

The RG equations for the Yukawa couplings in the various intermediate theories are collected in Appendix B. All our Yukawa-coupling results follow from the numerical integration of these equations with appropriate boundary conditions, though it is possible to make great progress in the analytic approximation of solutions to these equations. A systematic approximation scheme which reduces the solution to quadratures at each order of approximation is explained in Appendix B. The zeroth-order version of the scheme outlined in the Appendix produces accuracy of at least 5%, and often better, depending on the initial conditions. Unfortunately, this is not good enough for our purposes. We require accuracy comparable to the accuracy of the fermion masses, the worst case being the bottom-quark mass, conservatively known to within 3% (see Sec. V). Also, as explained in the Appendix, our approximate solutions lose all validity when the initial condition becomes large; thus we must use the full equations in order to calculate triviality bounds. Therefore, all analysis quoted here was done at the final stages by numerical integration of the equations; the analytical approximations were used only for guidance.

Within each of the symmetry-breaking chains exhibited above, there are two possible low-energy Higgs spectra; we can have either one or two light Higgs doublets, each deriving from the **10**, with the implied tree-level mass relation $m_b = m_\tau$.

In the case of one light Higgs doublet, some linear combination of the $(\mathbf{2},\mathbf{1})_1$ and $(\mathbf{2},\mathbf{1})_{-1}$ fields is assumed to be massive. This introduces an arbitrary mixing angle, which we denote by $\sin\theta$. In the case of two light Higgs doublets, there is also an extra parameter; this is the ratio of the vacuum expectation values (VEV's) for the two fields. The VEV's are denoted v_u and v_d, since one of the Higgs fields couples to "up-type" fermions, the top and the neutrino, and the other couples to "down-type" fermions, the bottom and the τ. The ratio is denoted by $\tan\beta = v_u/v_d$. Thus, in either of the cases we must specify two pieces of information, an initial condition and an angle.

Neutrino masses in the low-energy limit of SO(10) are naturally small due to the seesaw mechanism; in fact, the seesaw mechanism for neutrino masses was first introduced in the content of SO(10) [22]. Right-handed neutrinos become massive at the scale M_{R_0}, where the condensation of the $(\mathbf{1},\mathbf{1})_{2,\pm 1}$ breaks lepton number by two units; the right-handed neutrino mass is a Majorana mass. A subsequent diagonalization of the neutrino mass matrix gives a heavy, mostly right-handed neutrino, with mass $= O(M_{R_0})$, and a light, mostly left-handed neutrino with mass $= O(m^2_{\text{Dirac}}/M_{R_0})$, which is identified as the neutrino of the standard model. Here m_{Dirac} is the mass induced by the Yukawa coupling of the $(\mathbf{2},\mathbf{1})_{\pm 1}$, the standard-model Higgs doublet(s). A Majorana scale on the order of $10^{12}-10^{13}$ GeV, a typical value in SO(10), and a Dirac mass on the order of the Dirac mass of a generational counterpart fermion gives a physical neutrino mass which is safe cosmologically [23] and which can provide interesting physics, for example, a solution of the solar-neutrino problem [24–27] via Mikheyev-Smirnov-Wolfenstein (MSW) mixing [28,29].

The Yukawa couplings for the effective theories are as follows:

$$
\begin{aligned}
&G_{213}^{1\,\text{Higgs}}:\ h_t \bar{Q}_L \phi t_R + h_b \bar{Q}_L \tilde{\phi} b_R + h_\tau \bar{L}_L \tilde{\phi} \tau_R \ ,\\
&G_{213}^{2\,\text{Higgs}}:\ h_t \bar{Q}_L \phi_u t_R + h_b \bar{Q}_L \phi_d b_R + h_\tau \bar{L}_L \phi_d \tau_R \ ,\\
&G_{2113}^{1\,\text{Higgs}}:\ h_t \bar{Q}_L \phi t_R + h_b \bar{Q}_L \tilde{\phi} b_R + h_\tau \bar{L}_L \tilde{\phi} \tau_R\\
&\qquad\qquad + h_\nu \bar{L}_L \phi \nu_R + h_\Phi \bar{\nu}_R \nu_R^c \Phi \ ,\\
&G_{2113}^{2\,\text{Higgs}}:\ h_t \bar{Q}_L \phi_u t_R + h_b \bar{Q}_L \phi_d b_R + h_\tau \bar{L}_L \phi_d \tau_R\\
&\qquad\qquad + h_\nu \bar{L}_L \phi_u \nu_R + h_\Phi \bar{\nu}_R \nu_R^c \Phi \ ,\\
&\Phi = \Phi(\mathbf{1},\mathbf{1})_{2,1}\ , G_{2213}:\ h_q \bar{Q}_{iL} \phi_{ij} Q_{jL} + h_l \bar{L}_{iL} \phi_{ij} L_{jR}\\
&\qquad\qquad + h_\Phi \bar{\nu}_R \Phi \nu_R^c \ ,\\
&\Phi = \Phi(\mathbf{1},\mathbf{3},\mathbf{1})_2 \ ,\\
&\phi_{ij} = \phi(\mathbf{2},\mathbf{2},\mathbf{1})_0 \ .
\end{aligned}
\tag{4.1}
$$

The boundary conditions for the Yukawa couplings at the intermediate scales are as follows.

One-Higgs-doublet case:

$$
\begin{aligned}
&G_{213} \leftarrow G_{2113}:\ \text{continuity}\ ,\\
&G_{2113} \leftarrow G_{2213}:\ h_\tau/h_b = h_\nu/h_t\ ,\\
&\qquad h_l^2 = h_\nu^2 + h_\tau^2,\quad h_q^2 = h_t^2 + h_b^2\ ,\\
&G_{2113} \leftarrow G_{214}:\ h_b = h_\tau = h_u \cos\theta\ ,\\
&\qquad h_t = h_\nu = h_u \sin\theta\ ,\\
&G_{2213} \leftarrow G_{224}:\ h_q = h_l = h_u\ .
\end{aligned}
\tag{4.2}
$$

Two-Higgs-doublet case:

$$
\begin{aligned}
&G_{213} \leftarrow G_{2113}:\ \text{continuity}\ ,\\
&G_{2113} \leftarrow G_{2213}:\ h_t = h_b = h_q,\quad h_\nu = h_\tau = h_l\ ,\\
&G_{2113} \leftarrow G_{214}:\ h_t = h_b = h_\tau = h_\nu = h_u\ ,\\
&G_{2213} \leftarrow G_{224}:\ h_q = h_l = h_u\ .
\end{aligned}
\tag{4.3}
$$

When the effective theory is the standard model, with either one or two Higgs doublets, there are three independent Yukawa couplings in the top generation: h_t, h_b, and h_τ. In the two-Higgs-doublet model, the up-type fermions (top) couple to the Higgs field that we will call ϕ_u, and the down-type fermions (bottom and τ) couple to the Higgs field that we will call ϕ_d. In the one-Higgs-doublet model, only the linear combination $\phi = \sin\theta\phi_u + \cos\theta\phi_d$ is light; however, at the level of couplings of representations it is useful to imagine the couplings as being again to ϕ_u and ϕ_d; this simplifies the comparison between the two-Higgs-doublet and one-Higgs-doublet cases at the illustrative level. In the G_{2113} theory we introduce another Dirac-Yukawa coupling for the neutrino, and we also introduce the coupling of the ν_R to the $(\mathbf{1},\mathbf{1})_{2,1}$. In the G_{2213} theory the quarks and leptons have separate couplings to the $(\mathbf{2},\mathbf{2},\mathbf{1})_0$ bidoublet. Finally, $SU(4)_c$ is restored above M_c, and the Yukawa couplings must unify.

For later reference we note that we can write the muon-neutrino mass as

$$m_{\nu_\mu} = \left[\frac{h_{\nu_\mu}}{h_c} \right]^2 \frac{m_c^2}{h_\Phi M_{R_0}}$$
$$\simeq 0.6 \text{ eV} \left[\frac{h_{\nu_\mu}}{h_c} \right]^2 \frac{10^{10} \text{ GeV}}{h_\Phi M_{R_0}} . \quad (4.4)$$

Though we do not calculate generational mixing in this paper, we can estimate the Dirac-Yukawa couplings h_{ν_μ} and h_c by the same code as is used for the heavy-generation Yukawa RG flows. We know, for example, that $h_{\nu_\mu} < h_c$ by the same argument as is given below for the inequality $h_{\nu_\tau} < h_t$. We are interested in m_{ν_μ} because it must lie in a specific range 3×10^{-4} eV $< m_{\nu_\mu} < 10^{-2}$ eV [29,25] if we desire to solve the solar-neutrino problem via MSW mixing between ν_e and ν_μ. We have assumed that $m_{\nu_e} \ll m_{\nu_\mu}$, which is the situation in SO(10). By comparison with Eq. (4.4), Ref. [26] gives $m_{\nu_\mu} \simeq (0.3)^2 m_c^2 / h_\Phi M_{R_0}$, which is confirmed at the 25% level by our numerical analysis.

V. THE ONE-HIGGS-DOUBLET CASE

Consider first the case of a one-Higgs-doublet standard model embedded in SO(10). As outlined above, there are ten parameters which we imagine varying: the fermion masses m_t, m_b, m_τ; the Dirac-Yukawa coupling of the neutrino at the lepton-number-violating scale, $h_\nu(M_{R_0})$; the mass scales M_{R_0} and M_{R_+}; $\alpha_3(M_Z)$; $\sin^2\theta_W$; the unified Yukawa coupling h_u; and either $\sin\theta$ or $\tan\beta$. There is also the neutrino Majorana-Yukawa coupling h_Φ, which descends from the Yukawa coupling of the **126** at the unification scale, but it is easy to parametrize the effect of this coupling. We have determined that its effect on the fermion Dirac masses is negligible; the solutions to the Yukawa RG equations for the Dirac-Yukawa couplings are sensitive to its value only at the level of 1% or less. The only non-negligible effect of this coupling is, of course, in the determination of the physical neutrino mass through the seesaw mechanism, $m_\nu \simeq m_{\text{Dirac}}^2 / h_\Phi M_{R_0}$. Thus, by expressing our results in terms of the scale $h_\Phi M_{R_0}$ we can remove this extra degree of freedom.

The boundary conditions for the RG equations give four conditions on the ten parameters above. Our procedure is to fix $m_t, m_\tau, M_{R_0}, M_{R_+}, \alpha_3(M_Z)$, and $\sin^2\theta_W$ and obtain $m_b, h_\nu(M_{R_0}), h_u$, and $\sin\theta$ or $\tan\beta$; the parameters $\sin\theta$ or $\tan\beta$ are not of interest to us, and h_u is of interest only when it is forced to be large. We obtain curves of m_b and $h_\nu(M_{R_0})$ as functions of m_t for fixed values of the other parameters. Then by varying $\alpha_3(M_Z)$ and $\sin^2\theta_W$ over their quoted ranges we obtain our constraints. In practice the uncertainty in $\alpha_3(M_Z)$ gives the greatest contribution to the error, not only because its error is the largest fractionally, but because of the importance of the strong coupling in the running of the quark masses. As nominal values for the measured parameters, we choose

$$\begin{aligned} &m_b(m_b) = 4.25 \pm 0.10 \text{ GeV} , \\ &\alpha_3(M_Z) = 0.113 \pm 0.01 , \\ &\sin^2\theta_W = 0.233 \pm 0.002 , \\ &m_\tau = 1.784^{+0.0027}_{-0.0036} \text{ GeV} . \end{aligned} \quad (5.1)$$

The definition of m_b is as discussed in [30]. This mass is the running quark mass in the modified minimal subtraction ($\overline{\text{MS}}$) scheme. Higher values of m_b are derived in potential models [31], but these constituent quark masses are not the appropriate quantities for our analysis. Note that we will attempt to state all our results in a way that does not hide the dependence on m_b, since, as we will see, this is a critical parameter.

The value of $\sin^2\theta_W$ is an average of measurements in [1]. The central value for $\alpha_3(M_Z)$ is that obtained by a new analysis of jet shape distributions from the CERN e^+e^- collider LEP [32], and is somewhat lower than previous estimates. If one feels that this choice is suspect, then it is reassuring to note that higher values of $\alpha_3(M_Z)$ tend to make our derived constraints stronger since they imply larger values for h_b, making the agreement with the measured m_b worse.

As demonstrated for the simplest symmetry-breaking scheme [5], it can be difficult to accommodate the known fermion masses into this model as a low-energy limit of SO(10), since it is difficult to reconcile the large top-quark–bottom-quark splitting with unification when there is only one low-energy VEV determining both masses.

The current bounds on the top-quark mass which we use are $m_t > 91$ GeV (95% C.L.) from direct search [4] and $m_t < 182$ GeV (95% C.L.) calculated from the constraint on the measured value of the ρ parameter for the one-Higgs-doublet model [33]. Together with this bound, we also have strong constraints on the mass of the τ neutrino. The direct limit on the τ-neutrino mass is currently $m_{\nu_\tau} < 35$ MeV [34]. Cosmology provides a strong constraint in a large window just below the direct limit. The analysis of [35] shows that we must demand $m_{\nu_\tau} \lesssim 65$ eV or 1 MeV $\lesssim m_{\nu_\tau} \lesssim 35$ MeV in order to be consistent with the constraint on the observed energy density of the Universe, $\Omega \lesssim 1$, and the success of primordial nucleosynthesis. Clearly, because of the nature of the constraint on m_{ν_τ}, the unexcluded region in the (M_{R_0}, M_{R_+}) plane will consist of two bands: one near $M_{R_0} \simeq 10^6$ GeV and one above $M_{R_0} \simeq 10^{11}$ GeV. The detailed nature of these bands, at the level of a factor ~ 1 to 10 in the intermediate scales, depends on the values of the Yukawa couplings as determined by the RG flows.

In Fig. 2 we show the excluded region for various conditions on m_b for the value of $\alpha_3(M_Z)$ giving the weakest constraint, using the above limits on m_t and $m_{\nu\tau}$. For $\alpha_3(M_Z) \gtrsim 0.113$, the whole of the one-Higgs-doublet case becomes unviable. The exclusions take into account the 1σ variation of $\sin^2\theta_W$. A typical curve for m_b as a function of m_t, with other parameters fixed, is shown in Fig. 3. We see that m_b for fixed m_τ is not very sensitive to the

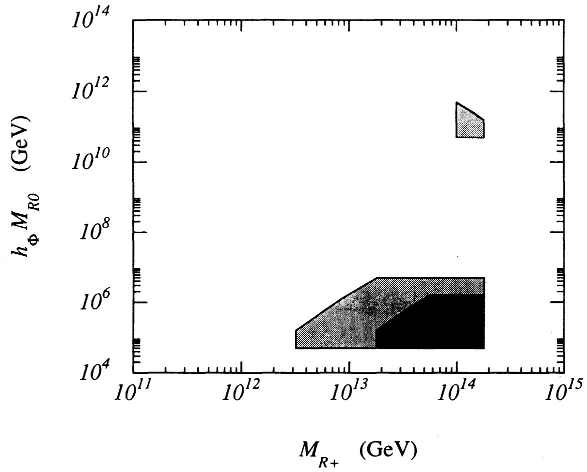

FIG. 2. Exclusion plot in the (M_{R_+}, M_{R_0}) plane for the one-Higgs-doublet case. The region near the top of the plot is excluded by obvious inequalities among the scales. The darker region is the allowed region for $m_b = 4.25 \pm 0.10$ GeV, and the lighter region is the allowed region for $m_b = 4.25 \pm 0.25$ GeV. 1σ variations in $\sin^2\theta_W$ are included in the analysis.

strength of the Yukawa couplings (represented through the top-quark mass) until the top quark is made quite heavy. This is because the RG equations for the τ and the bottom quark in the G_{213} stage (the standard model) admit an approximation rendering them linear, as explained in Appendix B. Because of the flatness of these relations and the uncertainty in m_b, it is not possible to give interesting bounds on m_t in most of parameter space. The effect on these curves of increasing $\alpha_3(M_Z)$ is generically to raise the values of m_b represented. Thus we see why higher values of $\alpha_3(M_Z)$ constrain the model more effectively. In Appendix B, some properties of the RG flow which lead to the qualitative features seen here are illustrated for the two-Higgs-doublet case. The one-doublet case behaves similarly, and is in fact somewhat

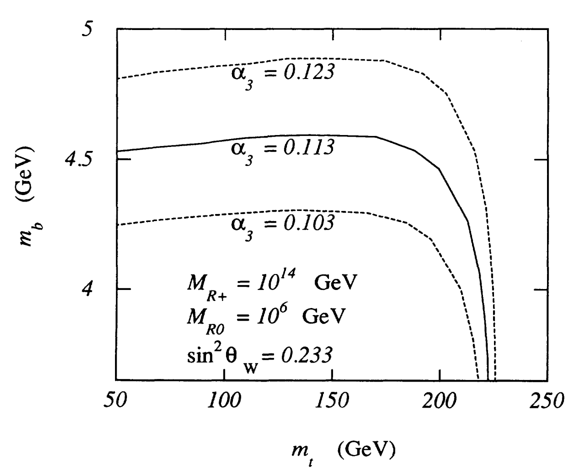

FIG. 3. m_b vs m_t, for varying $\alpha_3(M_Z)$ and other parameters fixed, in the one-Higgs-doublet case.

simpler to understand due to the existence of an analytic solution for the standard-model regime, as also discussed in Appendix B.

The turnover behavior of $m_b(m_t)$ in Fig. 3 at large values of m_t indicates the "triviality bound" phenomenon for these RG equations. In other words, large values of the initial Yukawa coupling are required to generate these high values at low energies, since values which are large enough to make the β function positive are quickly damped as we move downward in energy [36]. This effect leads to a bound in the standard model, $m_t \lesssim 250$ GeV [37]; in our case the effect is more pronounced since, roughly speaking, the β functions of the intermediate theories are more positive than would be the naive extension of the standard-model β functions into the same energy regimes. This turnover phenomenon is obviously problematic; if one were willing to trust the analysis at large Yukawa couplings, then any lower value of m_b could be arranged by simply taking the initial Yukawa coupling as high as necessary. Fortunately, the ρ-parameter constraint makes this discussion academic in the one-doublet case, and this constraint accounts for a large fraction of the exclusion we have shown. Note that both in the one-doublet and two-doublet cases, our analysis extended only up to values of the unified Yukawa coupling beyond which it seems certain that perturbative corrections become large; for definiteness $h_u < 10$ or $h_u/4\pi \lesssim 0.8$.

The qualitative features of the exclusion plots are easily explained. The exclusions in the vertical direction (M_{R_0}) are due to the bounds on the τ-neutrino mass. The exclusions in the horizontal direction (M_{R_+}) are due to the bounds on m_b. This follows because, as we have noted above, the Yukawa-coupling β functions in the theories at higher energies are less negative than would be an extension of the standard-model β functions into those regions; thus there must be an increase in $\sin\theta$ in order to keep the τ mass fixed. This also results in an increase for the calculated value of m_b, so as to strengthen the constraint.

The Yukawa-coupling evolution is very insensitive to the choice of D-parity-breaking scale. Once this scale is set and the intermediate scales are calculated, the only way the D symmetry enters the evolution is through the form of the scalar contributions to the gauge-coupling evolution; the implicit effect on the Yukawa-coupling β functions is small. It is fair to say that this holds true for any of the scalar contributions; the scalars are important in the calculation of the intermediate scales, but that is the only significant way that they affect the Yukawa evolution in our models.

VI. THE TWO-HIGGS-DOUBLET CASE

Consider next the case of a two-Higgs-doublet standard model embedded in SO(10). The discussion above regarding D parity applies equally here, and we discuss it no further. Following the analyses of the one-Higgs-doublet case, we use the current constraints on m_t and m_{ν_τ} to generate an exclusion plot in the (M_{R_0}, M_{R_+})

plane. However, in the two-Higgs-doublet case we do not have the benefit of a strong ρ-parameter constraint; the ρ-parameter constraint in the two-Higgs-doublet standard model is significantly less stringent than that in the one-doublet model [38]. A constraint derived independently of the Higgs sector has been calculated in [33], where they find $m_t < 310$ GeV (95% C.L.); this does not provide a sufficient extra constraint for us. In fact, it is possible for us to give a much more stringent bound for m_t, valid over the whole (M_{R_0}, M_{R_+}) plane, which is the triviality bound for this incarnation of SO(10). We find $m_t < 210$ GeV. This bound, by its nature, is insensitive to m_b, and it is quite firm.

In Fig. 4 we show a typical curve for m_b as a function of m_t in the two-doublet case. Numerically, we find lower values of m_b in the two-doublet case than in the one-doublet case, fixing all other parameters. This is because the standard-model h_b β function is more positive in the two-doublet case than in the one-doublet case, as can be seen by examination of the coefficients of the Yukawa-coupling terms in these β functions. For lower values of the Yukawa couplings this difference disappears, but we operate in a regime where this effect is becoming important. The resulting lower values of m_b tend to accumulate near $m_b \simeq 4.3$ GeV, and this renders our method of constraint almost useless. Also, there is little solid external information which we can apply to further constrain the model. The exclusion plots for the two-Higgs-doublet case are shown in Fig. 5.

Furthermore, as evidenced by the triviality bound above, we find that the upper limit on m_t derived in [5] is relaxed, though we confirm the result of that analysis for values of the intermediate scales corresponding to the limited symmetry-breaking scheme considered there.

Some of the qualitative features of the RG flow which lead to the relations shown here are discussed in Appendix B (see Fig. 7 therein).

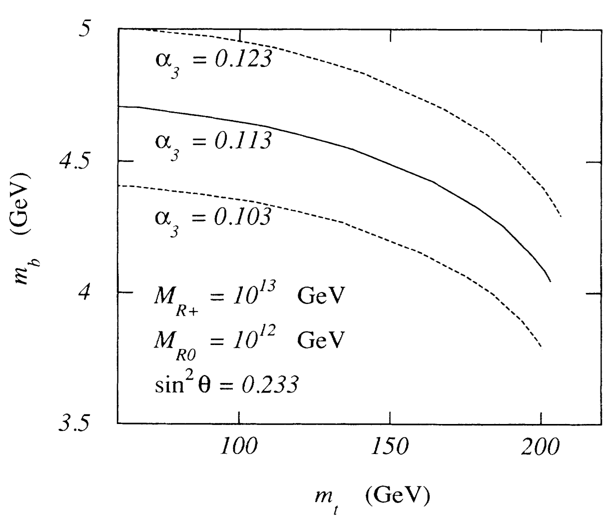

FIG. 4. m_b vs m_t, for varying $\alpha_3(M_Z)$ and other parameters fixed, in the two-Higgs-doublet case.

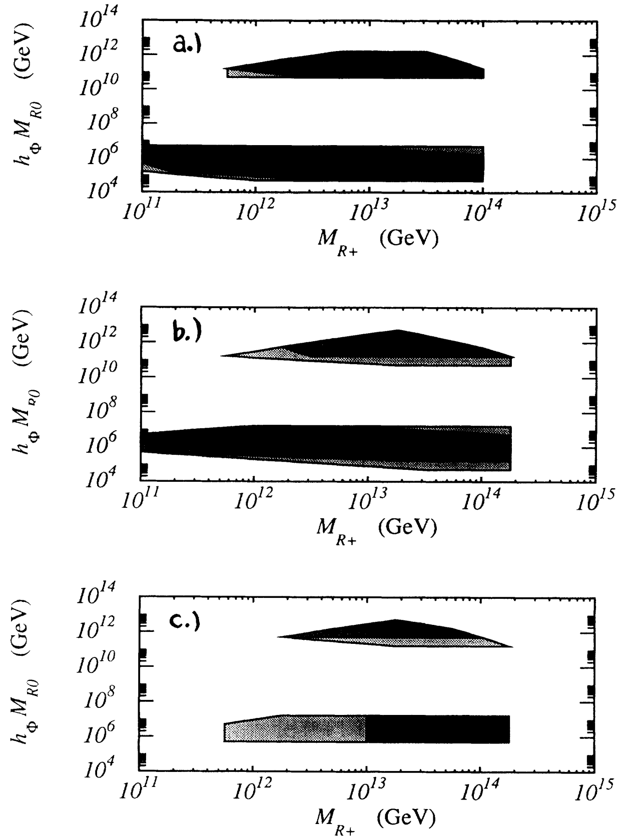

FIG. 5. Exclusion plots in the (M_{R_+}, M_{R_0}) plane for the two-Higgs-doublet case. The region near the top of the plot is excluded by obvious inequalities among the scales. The darker region is the allowed region for $m_b = 4.25 \pm 0.10$ GeV, and the lighter region is the allowed region for $m_b = 4.25 \pm 0.25$ GeV. (a) $\alpha_3 = 0.103$; (b) $\alpha_3 = 0.113$; (c) $\alpha_3 = 0.123$.

VII. A SECOND COSMOLOGICAL BOUND ON THE τ-NEUTRINO MASS

It has been suggested that the standard picture of neutrino mass generation in SO(10), in conjunction with anomalous $B+L$ violation at high temperatures, could lead to an unacceptable loss of baryons in the early Universe [7,8], violating the constraint from the observed baryon asymmetry [23]. This is because the condensation which gives rise to the Majorana-neutrino mass necessarily involves spontaneous violation of lepton number. Effective lepton-number-violating interactions, though suppressed by $m_{\nu,\mathrm{Dirac}}/M_{\Delta L}$, where $M_{\Delta L}$ is the Majorana scale, can combine with anomalous $B+L$ violation to wipe out baryon asymmetry in equilibrium. This is not a danger for the two lighter-generation neutrino couplings; however, the ν_τ can provide an effective interaction large enough that the rate for baryon-number depletion becomes problematic. Notice that the depletion of all baryon number requires adequate mixing between the generations, as discussed in [8]. Mixing questions are beyond the scope of this paper; we deal only with the heavy generation. However, we can calculate the appropriate Yukawa coupling $h_\nu(M_{R_0}); M_{R_0} = M_{\Delta L}$.

The example calculated in [8] to indicate the bound on M_{R_0} uses an implicit value for the Yukawa coupling $h_\nu(M_{R_0}) = \sqrt{2}$ in our normalization. This is actually somewhat large compared to typical values for this coupling in the SO(10) model, as indicated in our analysis. In particular, this coupling is comparable to the top-quark Yukawa coupling at the scale M_{R_0}, and as such it is significantly smaller than the top-quark coupling at the scale m_t since the Yukawa couplings rise as μ decreases over the range from M_{R_0} down to m_t. If one traces this Yukawa coupling through to the final bound, one finds that the bound has a strong dependence on its value:

$$h_\Phi \gtrsim \left[\frac{h_\nu}{\sqrt{2}} \right]^2 \frac{1}{50} \left[\frac{M_{\rm Pl}}{M_{R_0}} \right]^{1/2}$$

or $\qquad$ (7.1)

$$h_\nu \lesssim 0.3 h_\Phi^{1/2} \left[\frac{M_{R_0}}{10^{13}\ \text{GeV}} \right]^{1/4} .$$

How big can h_Φ be? Remember that its effect on the RG equations for the other Yukawa couplings is small; it is basically arbitrary, as long as it is not so big as to make its β function positive, violating its own triviality bound. So we can get an upper bound on h_Φ by finding that value for which its β function would necessarily become positive. Using typical values for the gauge couplings α_{BL} and α_{R_0}, we find $h_\Phi \lesssim 1.5$, a relatively small value since the gauge couplings of the Φ are weak. Therefore we cannot escape the bound (7.1) by raising h_Φ.

In Fig. 6 we have plotted $h_\nu(M_{R_0})$ as a function of m_t for the same parameter values which were used in Fig. 4. The relation between m_t and $h_\nu(M_{R_0})$ is linear at low couplings, as it should be, so that the bound (7.1) translates directly into a bound on m_t. Typically the bound (7.1) will correspond to a bound on the top-quark mass of $m_t \lesssim 100-130$ GeV. Looking at Figs. 6 and 4, we can see how the constraint on $h_\nu(M_{R_0})$ combines with that on m_b to eliminate regions of parameter space. Although the bound on m_t from the $h_\nu(M_{R_0})$ constraint $m_t \lesssim 125$ GV is itself not enough to cause concern, this constraint on m_t would require $m_b \gtrsim 4.5$ GeV for $\alpha_3(M_Z) = 0.113$, or conversely, would require $\alpha_3(M_Z) \lesssim 0.103$ to obtain an acceptable m_b. Thus the region of parameter space illustrated by Figs. 6 and 4 just barely qualifies as 1σ allowed.

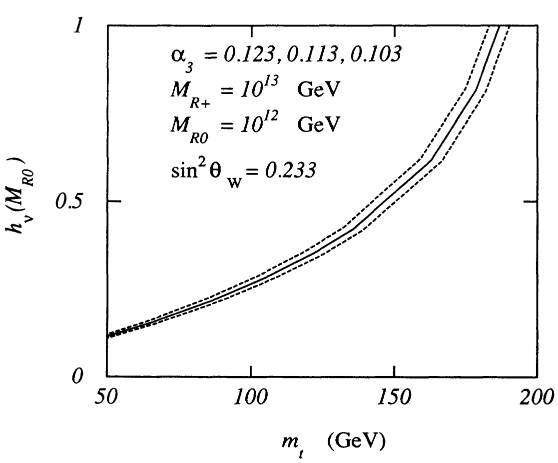

FIG. 6. $h_\nu(M_{R_0})$ vs m_t for the same fixed parameters as in Fig. 4.

Extending this sort of analysis over the whole of the parameter space we find that for $\alpha_3(M_Z) > 0.123$ both the one-Higgs-doublet and two-Higgs-doublet cases are ruled out. For $\alpha_3(M_Z) \lesssim 0.113$ the model is confined to the region $M_{R_0} > 8 \times 10^{12}$ GeV. Notice that the model is not completely ruled out, as one might have guessed by the dimensional analysis where one sets $h_\nu \simeq 1$. Consider the consequences of this result for the MSW mixing solution of the solar-neutrino problem. Using our expression for m_{ν_μ} in (4.4), we have

$$m_{\nu_\mu} \lesssim 7 \times 10^{-6}\ \text{eV} \left[\frac{h_{\nu_\mu}}{h_c} \right]^2 . \qquad (7.2)$$

If we run a one-generation Yukawa-coupling evolution for the second generation, we find $h_{\nu_\mu}/h_c \simeq 0.4$. As we noted previously, we expect this ratio to be less than 1, and from experience with the heavy-generation Yukawa-coupling evolution a value $\simeq \frac{1}{2}$ is sensible. Thus, we find $m_{\nu_\mu} \lesssim 10^{-4}$ eV, and the MSW mixing solution of the solar-neutrino problem is in grave jeopardy.

The constraint which we have derived here is, of course, somewhat speculative. A multigenerational analysis is required, both to understand the low-energy mixing angles and to estimate the muon-neutrino mass more accurately.

VIII. CONCLUSION

We have seen how Yukawa-coupling-constant unification together with the known bounds on fermion masses in the heavy generation are used to constrain the SO(10) model. The one-Higgs-doublet case is already severely constrained, and strenthening of these constraints can be foreseen for the near future, via improved measurements of $\sin^2\theta_W$ and especially of $\alpha_3(M_Z)$. The two-Higgs-doublet case is less constrained, and it seems from the analysis that progress in this case will be more difficult since what is really required here is an improvement in the estimate of m_b, something which is farther from us now than improvements in measurements of gauge-coupling constants.

The implications of SO(10) for neutrino physics have been very attractive for a number of years. However, as we saw in the last speculative section, it may be that the basic attractive feature of the model, naturally light seesaw masses from the breaking of intermediate $U(1)_{I_{3R}} \times U(1)_{B-L}$, will prove to scar another attractive feature, the ability to generate neutrino masses appropriate for MSW mixing. This issue can be settled by the calculation of flavor mixing in the lepton sector; one need only know whether or not the mixing is sufficient to drive interconversion among neutrino species with a high enough rate in the early Universe, so that the analysis may not be as complicated as could be a detailed study.

ACKNOWLEDGMENTS

The author would like to acknowledge encouraging and useful discussions with J. Rosner as well as with M. Booth and M. Luty.

APPENDIX A: HIGGS REPRESENTATIONS AND GAUGE-COUPLING EVOLUTION

In this Appendix we collect the quadratic Casimir constants for the intermediate Higgs representations as well as the equations for the evolution exponents which appear in Sec. III. Let $S_G(i)$ denote the quadratic Casimir constant for the Higgs representations occurring in the intermediate theory G, with respect to the gauge coupling α_i. Then the p and q exponents of Sec. III are given by the following.

Case $M_{R_+} < M_c$.

$$\begin{aligned}
p_u &= \tfrac{1}{44}[S_{224}(L)+S_{224}(R)-2S_{224}(4)] ,\\
p_+ &= \tfrac{1}{44}[S_{2113}(L)-S_{2213}(L)+S_{2113}(R_0)-S_{2213}(R)\\
&\quad +\tfrac{2}{3}S_{2113}(BL)-\tfrac{2}{3}S_{2213}(BL)] ,\\
p_0 &= \tfrac{1}{44}[S_{213}(L)-S_{2113}(L)+S_{213}(Y)\\
&\quad -S_{2113}(R_0)-\tfrac{2}{3}S_{2113}(BL)] ,\\
p_c &= \tfrac{1}{44}[S_{2213}(L)-S_{224}(L)+S_{2213}(R)-S_{224}(R)\\
&\quad +\tfrac{2}{3}S_{2213}(BL)+S_{224}(4)] ,\\
q_u &= \tfrac{1}{44}[3S_{224}(R)+2S_{224}(4)-5S_{224}(L)] ,\\
q_+ &= \tfrac{1}{44}[3S_{2113}(R_0)-3S_{2213}(R)+2S_{2113}(BL)\\
&\quad -2S_{2213}(BL)-5S_{2113}(L)+5S_{2213}(L)] ,\\
q_0 &= \tfrac{1}{44}[3S_{213}(Y)-5S_{213}(L)-3S_{2113}(R_0)\\
&\quad -2S_{2113}(BL)+5S_{2113}(L)] ,\\
q_c &= \tfrac{1}{44}[3S_{2213}(R)-3S_{224}(R)+2S_{2213}(BL)\\
&\quad -2S_{224}(BL)-5S_{2213}(L)+5S_{224}(L)] .
\end{aligned} \tag{A1}$$

Case $M_{R_+} > M_c$.

$$\begin{aligned}
p_u &= \tfrac{1}{44}[S_{224}(L)+S_{224}(R)-2S_{224}(4)] ,\\
p_+ &= \tfrac{1}{44}[S_{214}(L)-S_{224}(L)+S_{214}(R_0)\\
&\quad -S_{224}(R)+2S_{224}(4)-2S_{224}(4)] ,\\
p_0 &= \tfrac{1}{44}[S_{213}(L)-S_{2113}(L)+S_{213}(Y)\\
&\quad -S_{2113}(R_0)-\tfrac{2}{3}S_{2113}(BL)] ,\\
p_c &= \tfrac{1}{44}[S_{2113}(L)-S_{214}(L)+S_{2113}(R_0)-S_{214}(R_0)\\
&\quad +\tfrac{2}{3}S_{2113}(BL)+S_{214}(4)] ,\\
q_u &= \tfrac{1}{44}[3S_{224}(R)+2S_{224}(4)-5S_{224}(L)] ,\\
q_+ &= \tfrac{1}{44}[3S_{214}(R_0)-3S_{224}(R)+2S_{214}(4)\\
&\quad -2S_{224}(4)-5S_{214}(L)+5S_{224}(L)] ,\\
q_0 &= \tfrac{1}{44}[3S_{213}(Y)-5S_{213}(L)-3S_{2113}(R_0)\\
&\quad -2S_{2113}(BL)+5S_{2113}(L)] ,\\
q_c &= \tfrac{1}{44}[3S_{2113}(R_0)-3S_{214}(R_0)+2S_{2113}(BL)\\
&\quad -2S_{214}(BL)-5S_{2113}(L)+5S_{214}(L)] ,
\end{aligned} \tag{A2}$$

The quadratic Casimirs for the theories with D parity broken at the unification scale are

$$\begin{aligned}
&S_{213}(Y)=2N_D,\quad S_{213}(L)=\tfrac{3}{8}N_D ,\\
&S_{2113}(BL)=1,\quad S_{2113}(R_0)=1,\quad S_{2113}(L)=\tfrac{3}{8}N_D ,\\
&S_{2213}(BL)=3,\quad S_{2213}(R)=\tfrac{4}{3}+\tfrac{3}{4},\quad S_{2213}(L)=\tfrac{3}{4} ,\\
&S_{214}(4)=\tfrac{7}{15},\quad S_{214}(R_0)=10,\quad S_{214}(L)=\tfrac{3}{8}N_D ,\\
&S_{224}(4)=3+\tfrac{7}{15},\quad S_{224}(R)=\tfrac{22}{3}+\tfrac{3}{4},\quad S_{224}(L)=\tfrac{3}{4} ,
\end{aligned} \tag{A3}$$

where N_D is the number of Higgs doublets in the low-energy theory (the standard model). For the theories with unbroken D parity above the right-handed breaking scale we have

$$\begin{aligned}
&S_{224}(L)=S_{224}(R)=\tfrac{22}{3}+\tfrac{3}{4} ,\\
&S_{2213}(L)=S_{2213}(R)=\tfrac{4}{3}+\tfrac{3}{4} .
\end{aligned} \tag{A4}$$

APPENDIX B: THE YUKAWA-COUPLING RG EQUATIONS

In this Appendix we collect the RG equations for the Yukawa couplings of all the intermediate theories in the cases that interest us. We also discuss analytical approximation of the solutions, as mentioned in the text. The normalization of the Yukawa couplings was chosen such that "mass"="Yukawa"×174 GeV. We use the abbreviated notation

$$\mathcal{D}=16\pi^2\mu\frac{d}{d\mu} . \tag{B1}$$

Also, as an illustrative example of the Yukawa-coupling evolution, we include Fig. 7. This shows the evolution in the two-Higgs-doublet case for two values of the initial Yukawa coupling and illustrates the mechanism of the triviality bound as well as the behavior of m_b as a function of m_t for fixed m_τ.

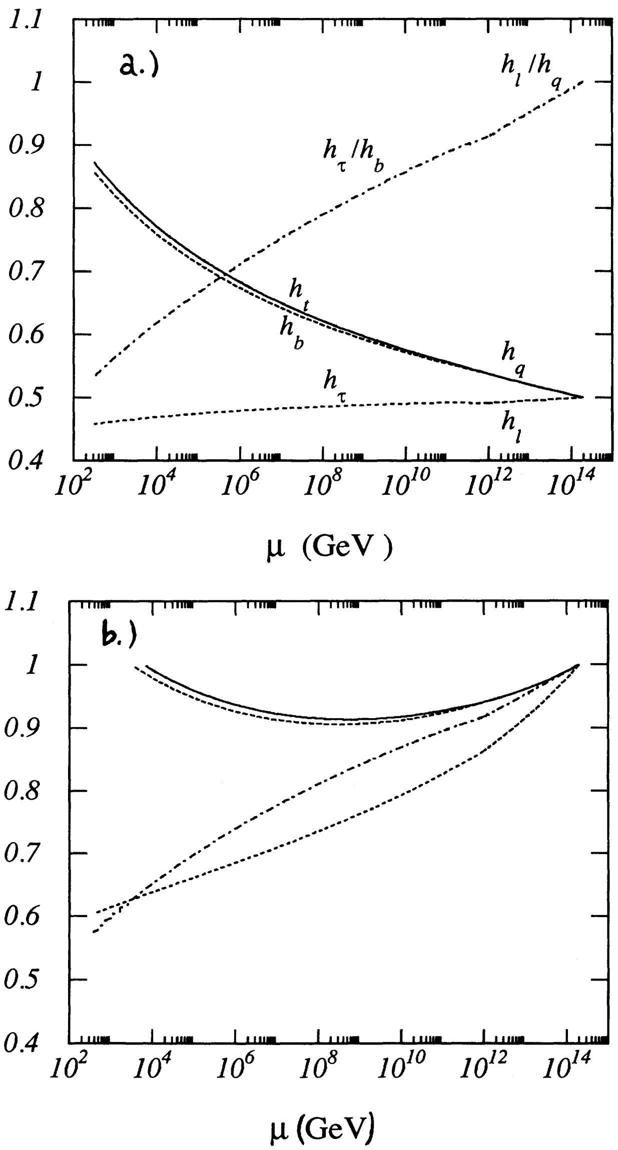

FIG. 7. Evolution of the Yukawa couplings for the two-doublet case, with $M_{R_+}=10^{12}$ GeV and $M_{R_0}=10^{11}$ GeV. (a) Evolution beginning with a unified coupling $h_u=0.5$; (b) Evolution beginning with a unified coupling $h_u=1.0$. Notice in particular the different qualitative behavior of the evolution for the large and small initial couplings; the saddle-shaped behavior in the second plot shows the mechanism for the triviality bound, near its onset as a function of the initial coupling. The curve labels in the second plot have been suppressed, being understood to be the same as in the first plot. The ratio h_τ/h_b has been shown in each plot in order to follow the evolution of the bottom-quark-Yukawa coupling at fixed m_τ. The endpoints of this family of curves generate the plots of m_b vs m_t for fixed m_τ, which are seen in the analysis of Secs. V and VI.

1. G_{213}, one Higgs doublet

These are the usual Yukawa-coupling RG equations for the standard model with one Higgs doublet [39]. The couplings are as defined in Sec. IV:

$$\begin{aligned}
&\mathcal{D}h_t^2=h_t^2(9h_t^2+3h_b^2+2h_\tau^2-2A_u)\,,\\
&\mathcal{D}h_b^2=h_b^2(9h_b^2+3h_t^2+2h_\tau^2-2A_d)\,,\\
&\mathcal{D}h_\tau^2=h_\tau^2(5h_\tau^2+6h_t^2+6h_b^2-2A_l)\,,\\
&A_u=4\pi(\tfrac{9}{4}\alpha_L+\tfrac{17}{12}\alpha_Y+8\alpha_3)\,,\\
&A_d=4\pi(\tfrac{9}{4}\alpha_L+\tfrac{5}{12}\alpha_Y+8\alpha_3)\,,\\
&A_L=4\pi(\tfrac{9}{4}\alpha_L+\tfrac{15}{4}\alpha_Y)\,.
\end{aligned}\tag{B2}$$

2. G_{2113}, one Higgs doublet

$$\begin{aligned}
&\mathcal{D}h_t^2=h_t^2(9h_t^2+3h_b^2+2h_\tau^2+2h_\nu^2-2A_u')\,,\\
&\mathcal{D}h_b^2=h_b^2(9h_b^2+3h_t^2+2h_\tau^2+2h_\nu^2-2A_d')\,,\\
&\mathcal{D}h_\tau^2=h_\tau^2(5h_\tau^2-h_\nu^2+6h_t^2+6h_b^2-2A_l')\,,\\
&\mathcal{D}h_\nu^2=h_\nu^2(5h_\nu^5-h_\tau^2+6h_t^2+6h_b^2+2h_\Phi^2-2A_\nu')\,,\\
&\mathcal{D}h_\Phi^2=h_\Phi^2(3h_\Phi^2+4h_\nu^2-2A_\Phi)\,,\\
&A_u'=4\pi(\tfrac{9}{4}\alpha_L+\tfrac{17}{20}\alpha_{R_0}+\tfrac{17}{30}\alpha_{BL}+8\alpha_3)\,,\\
&A_d'=4\pi(\tfrac{9}{4}\alpha_L+\tfrac{1}{4}\alpha_{R_0}+\tfrac{1}{6}\alpha_{BL}+8\alpha_3)\,,\\
&A_l'=4\pi(\tfrac{9}{4}\alpha_L+\tfrac{9}{4}\alpha_{R_0}+\tfrac{3}{2}\alpha_{BL})\,,\\
&A_\nu'=4\pi(\tfrac{9}{4}\alpha_L+\tfrac{9}{4}\alpha_{R_0}+\tfrac{3}{2}\alpha_{BL})\,,\\
&A_\Phi=4\pi(\tfrac{3}{2}\alpha_{BL}+\tfrac{9}{4}\alpha_{R_0})\,.
\end{aligned}\tag{B3}$$

3. G_{213}, two Higgs doublets

$$\begin{aligned}
&\mathcal{D}h_t^2=h_t^2(9h_t^2+h_b^2+2h_\tau^2-2A_u)\,,\\
&\mathcal{D}h_b^2=h_b^2(h_t^2+9h_b^2+2h_\tau^2-2A_d)\,,\\
&\mathcal{D}h_\tau^2=h_\tau^2(5h_\tau^2+6h_b^2-2A_l)\,.
\end{aligned}\tag{B4}$$

Here A_u, A_d, and A_l are as in the G_{213} one-Higgs-doublet case.

4. G_{2113}, two Higgs doublets

$$\begin{aligned}
&\mathcal{D}h_t^2=h_t^2(9h_t^2+h_b^2+2h_\nu^2-2A_u')\,,\\
&\mathcal{D}h_b^2=h_b^2(h_t^2+9h_b^2+2h_\tau^2-2A_d')\,,\\
&\mathcal{D}h_\tau^2=h_\tau^2(6h_b^2+5h_\tau^2+h_\nu^2-2A_l')\,,\\
&\mathcal{D}h_\nu^2=h_\nu^2(6h_t^2+h_\tau^2+5h_\nu^2+2h_\Phi^2-2A_\nu')\,.
\end{aligned}\tag{B5}$$

h_Φ, A_u', A_d', A_l', and A_Φ are as in the G_{2113} one-Higgs-doublet case.

5. G_{2213}

$$\begin{aligned}
\mathcal{D}h_q^2 &= h_q^2(10h_q^2+2h_l^2-2\overline{A}_q)\ ,\\
\mathcal{D}h_l^2 &= h_l^2(6h_q^2+6h_l^2+6h_\Phi^2-2\overline{A}_l)\ ,\\
\mathcal{D}h_\Phi^2 &= h_\Phi^2(5h_\Phi^2+4h_l^2-2\overline{A}_\Phi)\ ,\\
\overline{A}_q &= 4\pi(\tfrac{9}{4}\alpha_L+\tfrac{17}{20}\alpha_R+\tfrac{17}{30}\alpha_{BL}+8\alpha_3)\ ,\\
\overline{A}_l &= 4\pi(\tfrac{9}{4}\alpha_L+\tfrac{9}{4}\alpha_R+\tfrac{3}{2}\alpha_{BL})\ ,\\
\overline{A}_\Phi &= 4\pi(\tfrac{27}{8}\alpha_R+\tfrac{3}{2}\alpha_{BL})\ .
\end{aligned} \tag{B6}$$

6. Analytic approximation

It is possible to introduce a systematic approximation scheme for these Yukawa-coupling RG equations which, at zeroth order, provides solutions which are good to within about 5% or better, as long as highly nonlinear regions of the evolution are avoided. These are regions where the β functions become positive due to domination by the Yukawa-coupling terms over the gauge terms. This does not mean that Yukawa couplings must be small; it means only that they must be smaller than those values which will make the β functions positive. For example, such values occurred in the low-M_{R_0} allowed region for the one-Higgs-doublet model discussed in Sec. V above.

Let $y_i=h_i^2$. As a first step we note that the RG equations for the standard model with one Higgs doublet can be reduced to quadratures by the (excellent) approximation that h_b and h_τ are much smaller than h_t. With this approximation, the top RG equation decouples, and its solution is

$$y_t(t)=\frac{F_t^{213}(t)}{F_t^{213}(t_0)}\left[\frac{y_t(t_0)}{1-y_t(t_0)\dfrac{9}{16\pi^2}\displaystyle\int_{t_0}^{t}\frac{F_t^{213}(t)}{F_t^{213}(t_0)}}\right]\ , \tag{B7}$$

where

$$F_t^{213}(t)=\alpha_3(t)^{8/7}\alpha_L(t)^{27/40}\alpha_Y(t)^{-17/80}\ . \tag{B8}$$

The remaining equations are easily integrated by using the first equation to eliminate h_t. Their solutions are then given by

$$y_b(t)=y_b(t_0)\left[\frac{y_t(t)}{y_t(t_0)}\right]^{1/3}\left[\frac{\alpha_3(t)}{\alpha_3(t_0)}\right]^{16/21}\times\left[\frac{\alpha_L(t)}{\alpha_L(t_0)}\right]^{9/20}\left[\frac{\alpha_Y(t)}{\alpha_Y(t_0)}\right]^{1/120}\ , \tag{B9}$$

$$y_\tau(t)=y_\tau(t_0)\left[\frac{y_t(t)}{y_t(t_0)}\right]^{2/3}\left[\frac{\alpha_3(t)}{\alpha_3(t_0)}\right]^{-16/21}\times\left[\frac{\alpha_L(t)}{\alpha_L(t_0)}\right]^{9/40}\left[\frac{\alpha_Y(t)}{\alpha_Y(t_0)}\right]^{-101/240}\ . \tag{B10}$$

Notice that the α_3 dependence of y_τ is canceled by the leading factor in y_t, but the dependence on the nontrivial factor in parentheses in Eq. (B7) remains.

The RG equations for the remaining theories are less amenable to solution, since there is no obviously good approximation which decouples them. As an example of how to proceed we will analyze the equations for the standard model with two Higgs doublets. This will illustrate all the generic difficulties with this type of RG system and will illustrate our systematic approximation scheme for solutions. Let $Y(t)$ be a given (arbitrary) function. Consider the equations

$$\begin{aligned}
\frac{d}{dt}\ln y_t &= \frac{1}{16\pi^2}[9y_t+y_b+2Y+2\eta(y_\tau-Y)-2A_u]\ ,\\
\frac{d}{dt}\ln y_b &= \frac{1}{16\pi^2}[y_t+9y_b+2Y+2\eta(y_\tau-Y)\\
&\qquad -2A_u-2\eta(A_d-A_u)]\ ,\\
\frac{d}{dt}\ln y_\tau &= \frac{1}{16\pi^2}(5y_\tau+6y_b+y_t-2A_l)\ .
\end{aligned} \tag{B11}$$

When $\eta=1$ this system is the RG system given above for G_{213} with two Higgs doublets. When $\eta=0$ the first two equations decouple from the third. Notice that the driving gauge terms have been modified also, so that for $\eta=0$ the y_t and y_b equations are driven by the same function. This is an excellent approximation since A_u and A_d differ only in their α_Y terms, which are much smaller than the α_3 and α_L terms. The real problem with the $\eta=0$ equations is the replacement of y_τ with the given function $Y(t)$. $Y(t)$ can be anything, but we are wise to choose something which looks like y_τ. The simplest is to choose a constant such as $Y(t)=y_\tau(t_0)$. Since y_τ runs relatively slowly (absence of coupling to QCD), this works reasonably well. However, one could in principle do much better by choosing some more accurate approximation, such as $Y(t)=y_\tau(t_0)+(t-t_0)\dot{y}_\tau(t_0)+\cdots$, which is easily implemented since it requires no global information about y_τ. We find that with the constant choice, the solutions to the approximate system at zeroth order in η are good to 5% or better over a range of approximately 13 decades in energy, or $0<t\lesssim 30$. This is as long as one does not attempt to use the equations in the regions where β functions become large and positive; when this happens it means that the evolution is dominated by the nonlinear damping term, and the subsequent behavior is not modeled well by the zeroth-order approximant. However, note that this behavior can only occur over short intervals in t because of the damping effect as we flow towards the infrared.

At zeroth order in η it is straightforward to solve the reduced coupled system for y_t and y_b. Let $y_t=F(t)z_t$, $y_b=F(t)z_b$, where

$$F(t)=\exp\frac{1}{8\pi^2}\left[-\int_{t_0}^{t}dt\ A_u+\int_{t_0}^{t}Y\right]\ . \tag{B12}$$

Also, let $s(t)=\int_{t_0}^{t}F(t)$. Then after a little algebra the coupled system becomes

$$\frac{d\ln z_t}{d\ln z_b}=\frac{9z_t+z_b}{z_t+z_b}\ ,$$
$$\frac{d}{ds}\ln\frac{z_t}{z_b}=\frac{z_b}{2\pi^2}\left[\frac{z_t}{z_b}-1\right]\ . \tag{B13}$$

Introducing $v=z_t/z_b$, these become

$$\frac{dv}{\ln z_b}=8v\frac{v-1}{9+v}\ ,$$
$$\frac{d}{ds}\ln v=\frac{z_b}{2\pi^2}(v-1)\ . \tag{B14}$$

The first can be integrated, giving

$$z_b^8=C\frac{|v-1|^{10}}{v^9}\ , \tag{B15}$$

where we assumed without loss of generality that $v>1$. The second is reduced to a quadrature giving $v(s)$, and this combined with the definition of s gives the nearly complete reduction to quadratures. To complete the solution we can eliminate y_t and y_b from the y_τ equation and integrate that directly. Of course, evaluation of the quadratures can be subtle. All the integrals are expressible in terms of hypergeometric functions, but one must be careful that the requisite accuracy is maintained in the evaluation of these functions.

[1] DELPHI Collaboration, P. Abreu *et al.*, Nucl. Phys. **B367**, 511 (1991); OPAL Collaboration, G. Alexander *et al.*, Z. Phys. C **52**, 175 (1991); L3 Collaboration, B. Adeva *et al.*, *ibid.* **51**, 179 (1991); M. Martinez, Universitat Autonoma de Barcelona Report No. UAB-LFAE 91-03, 1991 (unpublished).

[2] U. Amaldi, W. de Boer, and H. Fürstenau, Phys. Lett. B **260**, 240 (1991).

[3] J. Ellis, S. Kelley, and D. V. Nanopoulos, Nucl. Phys. **B373**, 55 (1992); Phys. Lett. B **260**, 131 (1991).

[4] CDF Collaboration, F. Abe *et al.*, Phys. Rev. Lett. **68**, 447 (1992).

[5] E. M. Freire, Phys. Rev. D **43**, 209 (1991).

[6] G. Lazarides and Q. Shafi, Bartol Research Institute Report No. BA-89-67, 1989 (unpublished); Nucl. Phys. **B350**, 179 (1991).

[7] M. Fukugita and T. Yanagida, Phys. Rev. D **42**, 1285 (1990).

[8] J. Harvey and M. Turner, Phys. Rev. D **42**, 3344 (1990).

[9] G. Jungman (in preparation).

[10] H. Georgi and D. Nanopoulos, Nucl. Phys. **B159**, 16 (1979); R. N. Mohapatra and B. Sakita, Phys. Rev. D **21**, 1062 (1980); F. Wilczek and A. Zee, *ibid.* **25**, 553 (1982); R. N. Mohapatra, *Unification and Supersymmetry: The Frontiers of Quark-Lepton Physics* (Springer, New York, 1986).

[11] J. C. Pati and A. Salam, Phys. Rev. D **10**, 275 (1974); R. N. Mohapatra and J. C. Pati, *ibid.* **11**, 566 (1975); G. Senjanovic and R. N. Mohapatra, *ibid.* **12**, 1502 (1975).

[12] F. del Aguila and L. Ibanez, Nucl. Phys. **B177**, 60 (1981).

[13] R. N. Mohapatra and G. Senjanovic, Phys. Rev. D **27**, 1601 (1983).

[14] D. Chang, R. N. Mohapatra, and M. K. Parida, Phys. Rev. D **30**, 1052 (1984); D. Chang *et al.*, *ibid.* **31**, 1718 (1985).

[15] R. W. Robinett and J. L. Rosner, Phys. Rev. D **26**, 2396 (1982).

[16] V. V. Dixit and M. Sher, Phys. Rev. D **40**, 3765 (1989).

[17] IMB-3 Collaboration, R. Becker-Szendy *et al.*, Phys. Rev. D **42**, 2974 (1990).

[18] Y. Tosa, G. C. Branco, and R. E. Marshak, Phys. Rev. D **28**, 1731 (1983).

[19] V. A. Kuzmin and M. E. Shaposhnikov, Phys. Lett. **92B**, 115 (1980).

[20] D. Chang and R. N. Mohapatra, Phys. Rev. D **32**, 1248 (1985).

[21] T. P. Cheng, E. Eichten, and Ling-Fong Li, Phys. Rev. D **9**, 2259 (1974).

[22] M. Gell-Mann, P. Ramond, and R. Slansky, in *Supergravity*, Proceedings of the Workshop, Stony Brook, New York, 1979, edited by P. van Nieuwenhuizen and D. Freedman (North-Holland, Amsterdam, 1979); T. Yanagida, in *Proceedings of the Workshop on Unified Theories and Baryon Number in the Universe*, Tsukuba, Japan, 1979, edited by A. Sawada and A. Sugamoto (KEK Report No. 79-18, Tsukuba, 1979).

[23] E. Kolb and M. Turner, *The Early Universe* (Addison-Wesley, Reading, MA, 1989).

[24] J. N. Bahcall, W. F. Huebner, S. H. Lubow, P. D. Parker, and R. K. Ulrich, Rev. Mod. Phys. **54**, 767 (1982); J. N. Bahcall and R. K. Ulrich, *ibid.* **60**, 297 (1988).

[25] D. C. Kennedy, in Proceedings of the Theoretical Advanced Study Institute, Boulder, Colorado, 1990 (unpublished), p. 807.

[26] S. A. Bludman, D. C. Kennedy, and P. G. Langacker, Nucl. Phys. **B374**, 373 (1992).

[27] V. Barger, R. J. N. Phillips, and K. Whisnant, Phys. Rev. D **43**, 1110 (1991).

[28] L. Wolfenstein, Phys. Rev. D **17**, 2369 (1978); S. Mikheyev and A. Smirnov, Zh. Eksp. Teor. Fiz. **91**, 7 (1986) [Sov. Phys. JETP **64**, 4 (1986)].

[29] S. J. Parke, Phys. Rev. Lett. **57**, 1275 (1986).

[30] J. Gasser and H. Leutwyler, Phys. Rep. **87**, 77 (1982).

[31] C. Quigg and J. L. Rosner, Phys. Rev. D **23**, 2625 (1981); C. Quigg, W. Kwong, and J. L. Rosner, Annu. Rev. Nucl. Part. Sci. **37**, 325 (1987); H. Grosse and A. Martin, Phys. Rep. **60**, 341 (1980).

[32] J. Ellis, D. V. Nanopoulos, and D. A. Ross, Phys. Lett. B **267**, 132 (1991).

[33] P. Langacker and M. Luo, Phys. Rev. D **44**, 817 (1991).

[34] H. Albrecht *et al.*, Phys. Lett. B **202**, 149 (1988).

[35] H. Harari and Y. Nir, Nucl. Phys. **B292**, 251 (1987).

[36] For an account of "triviality bounds" and (quasi) fixed points for Yukawa RG equations, see J. Bagger, S. Dimopoulos, and E. Masso, Nucl. Phys. **B253**, 397 (1985).

[37] N. Cabibbo, L. Maiani, G. Parisi, and G. Petronzio, Nucl. Phys. **B158**, 295 (1979); J. Bagger, S. Dimopoulos, and E. Masso, Phys. Rev. Lett. **55**, 1450 (1985).

[38] A. Denner, R. J. Guth, and J. H. Kuhn, Phys. Lett. B **240**, 438 (1990).

[39] E. Ma and S. Pakvasa, Phys. Rev. D **20**, 2899 (1979).

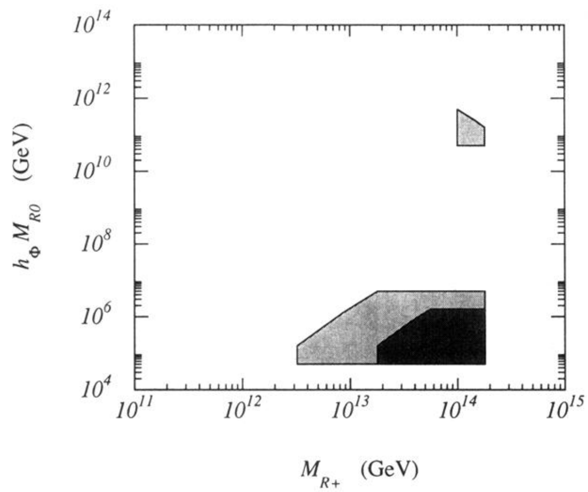

FIG. 2. Exclusion plot in the (M_{R_+}, M_{R_0}) plane for the one-Higgs-doublet case. The region near the top of the plot is excluded by obvious inequalities among the scales. The darker region is the allowed region for $m_b = 4.25 \pm 0.10$ GeV, and the lighter region is the allowed region for $m_b = 4.25 \pm 0.25$ GeV. 1σ variations in $\sin^2\theta_W$ are included in the analysis.

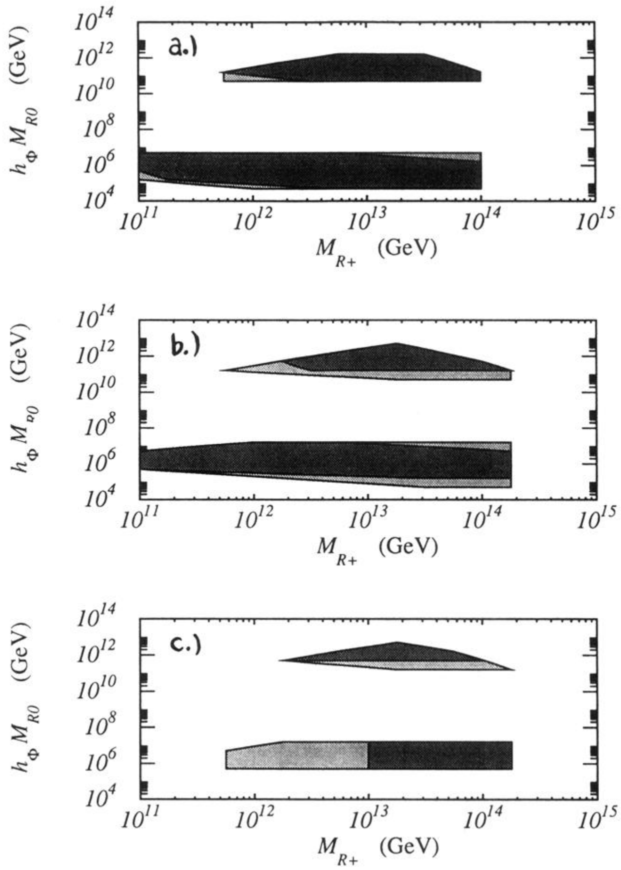

FIG. 5. Exclusion plots in the (M_{R_+}, M_{R_0}) plane for the two-Higgs-doublet case. The region near the top of the plot is excluded by obvious inequalities among the scales. The darker region is the allowed region for $m_b = 4.25 \pm 0.10$ GeV, and the lighter region is the allowed region for $m_b = 4.25 \pm 0.25$ GeV. (a) $\alpha_3 = 0.103$; (b) $\alpha_3 = 0.113$; (c) $\alpha_3 = 0.123$.